ELSEVIER

Journal of Applied Geophysics 48 (2001) 67–81

JOURNAL OF APPLIED GEOPHYSICS

www.elsevier.com/locate/jappgeo

Magnetic properties of salt-marsh soils contaminated by iron industry emissions (southeast France)

Hélène Lecoanet [a,*], François Lévêque [b], Jean-Paul Ambrosi [a]

[a] *CEREGE-UMR6635, Europôle de l'Arbois, BP 80, 13545 Aix en Provence cedex 04, France*
[b] *Centre Littoral de Géophysique, Avenue M. Crépeau, 17042 La Rochelle cedex 01, France*

Abstract

Detailed magnetic properties of salt-marsh soils exposed to intense atmospheric deposition of fly ashes from the iron industry (southeast France) are reported. An enhancement in the concentration of magnetic particles in topsoil through this area is observed. Low values of frequency-dependent susceptibility (χ_{FD}) are characteristic of coarse multidomain (MD) grains and were observed in surface samples. Concentration of ferrimagnetic minerals in different soil horizons is linked to pollution sources and the prevailing wind direction. The anhysteretic remanent magnetisation/saturation anhysteretic remanent magnetisation ($ARM_{40\ mT}$/SARM) ratio versus isothermal remanent magnetisation/saturation isothermal remanent magnetisation ($IRM_{-100\ mT}$/SIRM) ratio and the $IRM_{-20\ mT}$/SIRM ratio versus $IRM_{-200\ mT}$/SIRM ratio can differentiate two different contamination emission sources. Magnetic methods used reflect not only the concentration of ferrimagnetic minerals but also their grain size, thus enabling discrimination of metallurgical dusts and fine pedogenic particles created in situ. Our results suggest that pollution is not the only source and that pedogenesis also plays a role.
© 2001 Elsevier Science B.V. All rights reserved.

Keywords: Magnetic parameters; Iron industry; Atmospheric dust; Pedogenesis; Salt-marsh soil

1. Introduction

Several mechanisms can explain the enrichment in ferrimagnetic minerals in soils, for instance, long-term weathering and pedogenesis that can concentrate iron-bearing minerals (Singer and Fine, 1989). Some authors suggested the possibility of using magnetic susceptibility measurements in monitoring various features and properties of soils (Fine et al., 1992; Hunt et al., 1984; Maher, 1986). In addition, airborne magnetic particles mainly from pollution sources can also accumulate in soils (Hay et al., 1997). Thompson and Oldfield (1986) noted that soil close to large towns and industrial centres can have higher susceptibility than elsewhere. Metallurgical and industrial dusts and fly ashes contain magnetite. Therefore, these industries are directly responsible for the increase in the magnetic susceptibility of topsoil horizons (Hansen et al., 1981; Mitchell and Sluskoter, 1976). Magnetic measurements on soils can thus be used to determine the contributions from iron industry (Petrovsky and Ellwood, 1999; Durza, 1999; Heller et al., 1998; Strzyszcz and Magiera, 1996). Moreover, the anthropogenic or natural origin

* Corresponding author. Tel.: +33-4-4297-1581; fax: +33-4-4297-1549.
E-mail address: lecoanet@cerege.fr (H. Lecoanet).

0926-9851/01/$ - see front matter © 2001 Elsevier Science B.V. All rights reserved.
PII: S0926-9851(01)00080-5

of ferrimagnetic soil particles can be differentiated by investigating their magnetic domain state. Mullins (1977) demonstrated that pedogenic ferrimagnetic minerals consist of a mixture of superparamagnetic (SP) and single-domain (SD) grains.

Many anthropogenic aerosols are known to have a significant magnetic component (e.g. Kapicka et al., in press), but there are not that many studies dealing with their magnetic properties in detail (e.g. Shu et al., in press; Flanders, 1994, 1999; Dekkers and Pietersen, 1992). The present study examines the question which magnetic parameters or combination of parameters are the most useful to characterise soils and aerosol samples containing mixtures of anthropogenic magnetic minerals.

2. Sampling and methods

2.1. Site description

The area investigated located on the large grounds of a metallurgical plant in southeast France (Fig. 1) is approximately 1 km^2. Two sources of magnetic particle minerals exist (Fig. 2) to the north and to the west. As the main wind (mistral) is a northwest wind, the region is directly in the path of industrial dust fallout.

The northern part is a salt-marsh crossed by a drainage channel. The soils can be assigned to halomorphic anthroposoils (Baize and Rossignol, 1995; Gaucher and Burdin, 1974). The solum is composed of hydraulic backfilling dating from the 1970s and influenced by the seasonal variations of the shallow watertable (Fig. 3).

2.2. Sampling

In June 1998, magnetic susceptibility mapping was performed on 900 surface sites (crosses in Fig. 2), using a Bartington field probe MS2D. Each site is characterised by the same vegetal species (small grasses). At each site, three measurements were done to ensure repeatability and representativeness.

The resulting map was then used to choose six soil profiles (B, D, E, H, I, K) across the study area

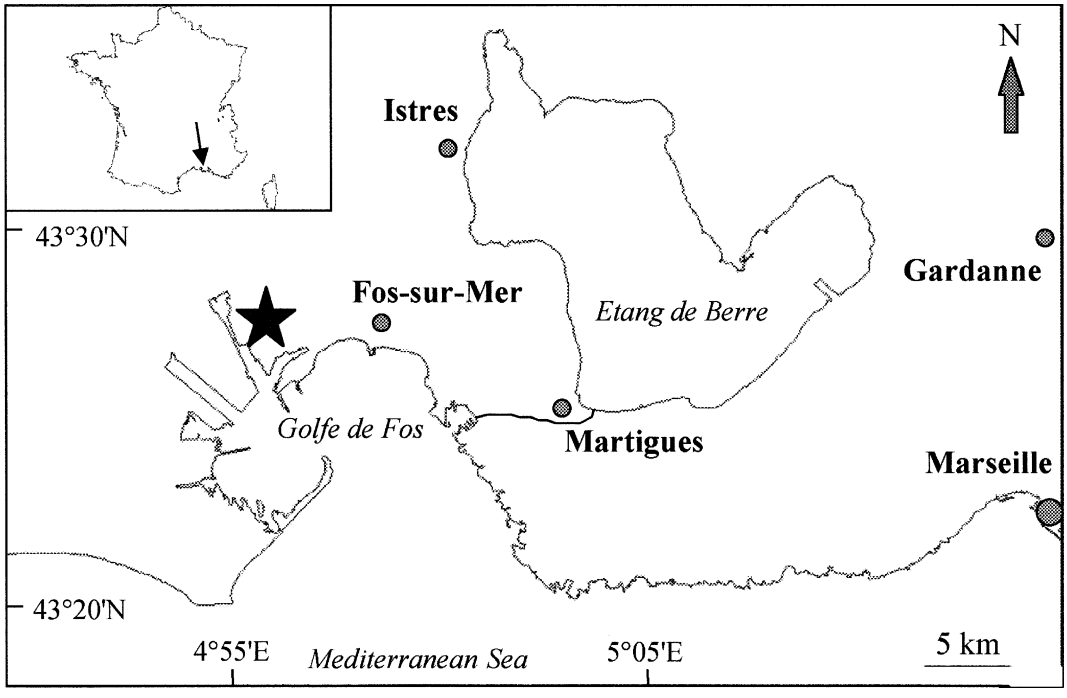


Fig. 1. Location map. Star symbol represents the studied area.

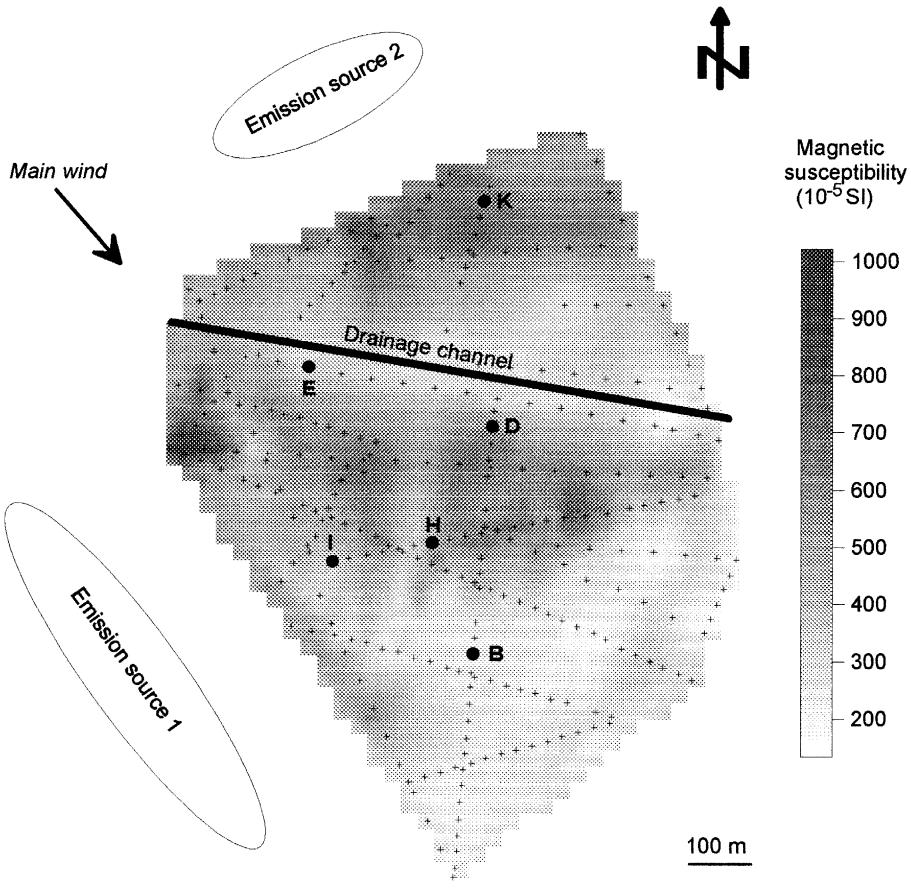


Fig. 2. Magnetic susceptibility map of topsoils. Crosses symbolise each surface measurement site. The gridding method selected is a triangulation with linear interpolation (Surfer 6.0 for Windows software). The six profiles are located with black rings and labelled B, D, E, F, I and K.

(Fig. 2) for further measurements in July 1998. Sixty-four soil samples were collected from a depth of 40 cm. In order to avoid any contamination, samples were collected from surface to bottom and put in situ into 8-cm^3 plastic boxes. Samples were stored in a cool place until analysis. After magnetic measurements, samples were air-dried and weighted.

At each profile sampling site, atmospheric dust was collected during a week between January and July 7, 1999 following the French standard NF X43.00 (Afnor, 1973). Stainless steel plaques were fixed horizontally at 1.5 m high. Atmospheric particles were collected on a 50-cm^2 surface and trapped with methyl-polysiloxan. In the laboratory, plaques were washed with dichloromethan. Particles were sorted by filtration (Whatman fibreglass filters, 1 μm), and the mass of fallout was determined by weight. Magnetic measurements were performed on folded filters fixed in the centre of 8-cm^3 plastic boxes.

2.3. Measurements

Magnetic susceptibility is linked directly to concentrations of ferrimagnetic minerals and is dominated by magnetite. Magnetic susceptibility expresses the ease at which materials can be magnetised. In our case, susceptibility measurements of surface soil samples were performed using a Bartington field probe MS2D (Bartington Instruments). The probe responds to the concentration of ferrimagnetic

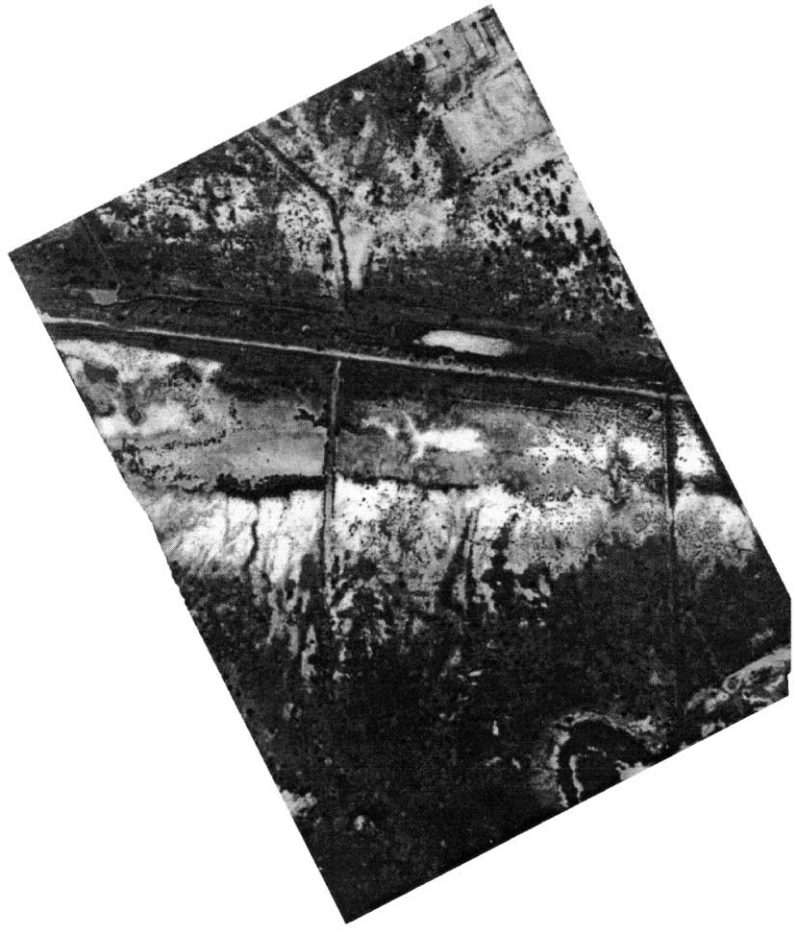


Fig. 3. Aerial photography of mapped area. Light colours means salt marsh areas. Scale: 1 cm to 100 m.

materials in the top 6–8 cm of soils (Lecoanet et al., 1999a; Dearing, 1994).

Field data were checked by laboratory susceptibility measurements on both soil samples and atmospheric dust filters using a Geofyzika KLY-2 Kappabridge. The intercalibration error between the KLY-2 Kappabridge and the MS2B probe is less than 2% (Lecoanet et al., 1999a).

Magnetic susceptibility was expressed in specific volume unit (κ, dimensionless) or specific mass unit (χ, $m^3\ kg^{-1}$). It is approximately proportional to the concentration of ferrimagnetic minerals such as iron oxides and hydroxides, iron sulphides, and also paramagnetic minerals like iron-bearing silicates.

Several other magnetic parameters were used to estimate grain-size distribution of the various sets of samples and concentration changes along profiles. For example, frequency-dependent susceptibility (Hanesch and Petersen, 1999; Forster et al., 1994; Dearing et al., 1996), anhysteretic remanent magnetisation (ARM) per unit field (Jordanova and Jordanova, 1999; Jordanova et al., 1997; Zhou et al., 1990) and normalised AF demagnetisation curves of ARM are commonly used to identify grain sizes and thus domain structure.

The Bartington laboratory probe MS2B measures low field magnetic susceptibility at two frequencies (χ_{LF} = 470 Hz and χ_{HF} = 4700 Hz) and can thus be

used to determine the possible presence of superparamagnetic (SP) mineral fraction using frequency-dependent susceptibility χ_{FD}: $\chi_{FD}\% = 100((\chi_{LF} - \chi_{HF})/\chi_{LF})$.

Viscous remanence magnetisation (VRM) was obtained after 15 days storage in a μ-metal shielded room (FD). The samples were then exposed to the Earth's magnetic field in a defined orientation during another period of 15 days (TR). The viscosity coefficient is then expressed as $Sv\% = 100((FD - TR)/FD)$.

Anhysteretic remanent magnetisation (ARM) was acquired during AC demagnetisation with amplitude decreasing from a maximum of 100 mT to zero, around a steady field $H_0 = 0.1$ mT, using a Schönstedt demagnetiser (Schönstedt Instrument, USA). χ_{ARM} is defined as the ratio ARM/H_0 ($m^3\ kg^{-1}$). The ARM acquired at 100 mT is called the saturation anhysteretic remanent magnetisation (SARM).

Isothermal remanent magnetisation (IRM) was acquired by placing samples in a steady field at room temperature and subsequently removing the field. A pulse magnetiser MMPM9 (Magnetic Measurements) was used. The IRM acquired at 2800 mT is called the saturation isothermal remanent magnetisation (SIRM). DC demagnetisation was carried out using the same field increment, with the field oriented against SIRM.

All remanent magnetisation measurements were performed along the *Z*-axis using a 2-G cryogenic magnetometer.

Finally, bivariant analyses (biplots), combining pairs of magnetic parameters acquired at room temperature (VRM versus κ, $ARM_{40\ mT}/SARM$ ratio versus $IRM_{-100\ mT}/SIRM$ ratio and $IRM_{-20\ mT}/SIRM$ ratio versus $IRM_{-200\ mT}/SIRM$ ratio), were used to identify ferrimagnetic minerals in soils and atmosphere dusts, and to determine possible contamination sources.

3. Results

3.1. Magnetic susceptibility mapping

Volume susceptibility values (κ) in topsoils can vary by over an order of magnitude. Magnetic susceptibility ranged from 104×10^{-5} to 1241×10^{-5} SI with a mean value of 431.4×10^{-5} SI (Fig. 2).

Low susceptibility values were measured in the southern part of the area and along the north side of the channel. In contrast, strongly magnetic soils overlying weakly magnetic substrates (quartzose sand) were found near the northern emission source and south of the drainage channel. Thus, we observed a strong variability of topsoil susceptibility values, whereas κ-normalised atmospheric fallout fluxes were nearly homogeneous over the entire area. In fact, the effect of dust fallout on the variability of susceptibility can be verified using a ratio of mass of collected dust (expressed in mass per unit area and unit time) and mass-specific magnetic susceptibility of collected dust samples (Fig. 4). This ratio shows slight variations with values (in arbitrary units) between 1.40 and 1.96, with a mean of 1.65. Therefore, topsoil susceptibility contrast may not only reflect atmospheric deposition of dust, varying with distance from metallurgical-dust source, but can also be due to in situ pedogenic transformation and salt-marsh plant zonation (Lecoanet et al., 1999b).

When comparing the magnetic susceptibility map with aerial photography (Fig. 3), it can be seen that high susceptibility values measured along the channel correspond to salt-affected soils (light areas in Fig. 3).

3.2. Soil profiles

3.2.1. Pedological description

The susceptibility map was used to select the location of soil profiles. Measurements were always

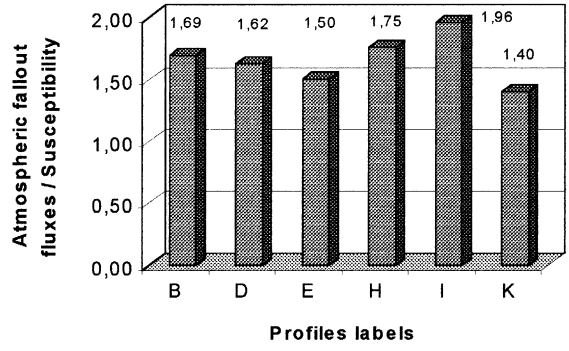


Fig. 4. Atmospheric fallout fluxes to volume susceptibility at each soil profile site.

made on the same vegetal species (small grasses) to minimise data acquisition errors. Therefore, profiles B, D, E, H, I and K were made under small grasses.

The topography of this area is fairly flat. All profiles are mainly composed of sandy material. Profiles D and I are localised in the salt-marsh area and contain clayey horizons. The transition between sandy and clayey horizons is often marked with oxidised strips. Only profile E contains a lot of pebbles of various sizes. The humic horizon is generally thin varying from 2.5 cm in profiles I, H, D to 5 cm in profiles B, E, K. Small roots were abundant in profiles E and K. Horizontal rhizomes were only observed in profiles H and I (Figs. 5.1 and 5.2).

X-ray analysis of surface soil samples showed that iron oxides (magnetite, maghemite and hematite) were present in all profiles, halite and gypsum in profiles D, H and I and pyrite in profiles B, D and H (see Table 1).

3.2.2. Magnetic measurements

3.2.2.1. Magnetic susceptibility. Along all the profiles, susceptibility values increase in topsoil (thin humic horizon) and decrease abruptly in the underlying soil horizons (Figs. 5.1 and 5.2).

The closer the profile to the source of pollution, the higher is the magnetic susceptibility, as shown by the susceptibility mapping (Fig. 2): κ is maximum at the top of profile K (2068×10^{-6} SI, Fig. 5.1) and minimum at the top of profile B (622×10^{-6} SI, Fig. 5.1). In mass specific units, χ is maximum at the top of profile D (12.4×10^{-6} m^3 kg^{-1}, Fig. 5.2) and minimum at the top of profile I (5.9×10^{-6} m^3 kg^{-1}, Fig. 5.2). These different results can be due to dilution effects or pedogenesis coming from the presence of varying organic matter content in surface samples.

High susceptibility values in topsoils seem to be correlated to metallurgical dust fallout, but pedogenesis could also explain such high concentrations of magnetic minerals (Maher, 1986; Fine et al., 1989).

3.2.2.2. Frequency-dependent susceptibility. Variation in susceptibility with frequency indicates the presence of grains lying at the stable single/superparamagnetic boundary. At higher frequencies of applied magnetic field, a portion of small SP grains is unable to follow the field changes and will no longer contribute to χ as superparamagnetic but as single-domain grains.

As predicted by Dearing's χ_{FD} model (Dearing et al., 1996), two types of magnetic assemblage can be identified in our samples. The majority of samples with a $\chi_{FD}\% < 2\%$ are dominated by frequency-independent coarse MD grains ($\chi_{FD}\%$ is even lower for topsoil samples): $< 0.1\%$ for profiles B, H, E, D and about 0.5% for profiles I and K (Figs. 5.1 and 5.2). The soil samples collected in clay horizons from profiles I and D (Fig. 5.2) belong to an intermediate group with $\chi_{FD}\%$ between 2% and 6%, corresponding to a mixture of frequency-dependent and independent grains. In our sample suite, no samples were dominated by frequency-dependent grains ($\chi_{FD}\% > 6\%$, dominant SP fraction).

Frequency-dependent susceptibility values of our samples do not span the whole range of 0–12% commonly observed in recent soils (Hanesch and Petersen, 1999; Magiera, 1998; Jordanova et al., 1997). $\chi_{FD}\%$ values measured in humic horizons range from 0% to 0.5% and are lower than values found by Heller et al. (1998) in the organic subhorizons from the Katowice province, which is similar to our study region in terms of character of pollution source and soil types. Thus, an additional presence of multidomain (MD) particles is assumed: magnetic susceptibility of our soils is controlled by aeolian metallurgical dusts of larger mean domain size.

3.2.2.3. χ_{ARM}/χ ratio. A gradual decrease in the χ_{ARM}/χ ratio is observed towards the upper part of humic horizons, particularly in profiles H and D (Fig. 5.2). This trend cannot reflect an SP enrichment because χ_{FD} (%) values are very low. Therefore, in the absence of SP, χ_{ARM}/χ ratio shows more likely a decrease in SSD (stable single-domain). Nevertheless, Jordanova et al. (1997) interpreted a local decrease of χ_{ARM}/χ at a level profile with a corresponding increase in χ as occasional SP enrichment.

Sand horizons are characterised by relatively constant values of the χ_{ARM}/χ ratio of about 4×10^{-6} SI. However at the sand–clay transition in profile I, χ_{ARM}/χ is 8.06×10^{-6} SI at -10 cm, and in profile D, χ_{ARM}/χ is 6.79×10^{-6} SI at -10 cm;

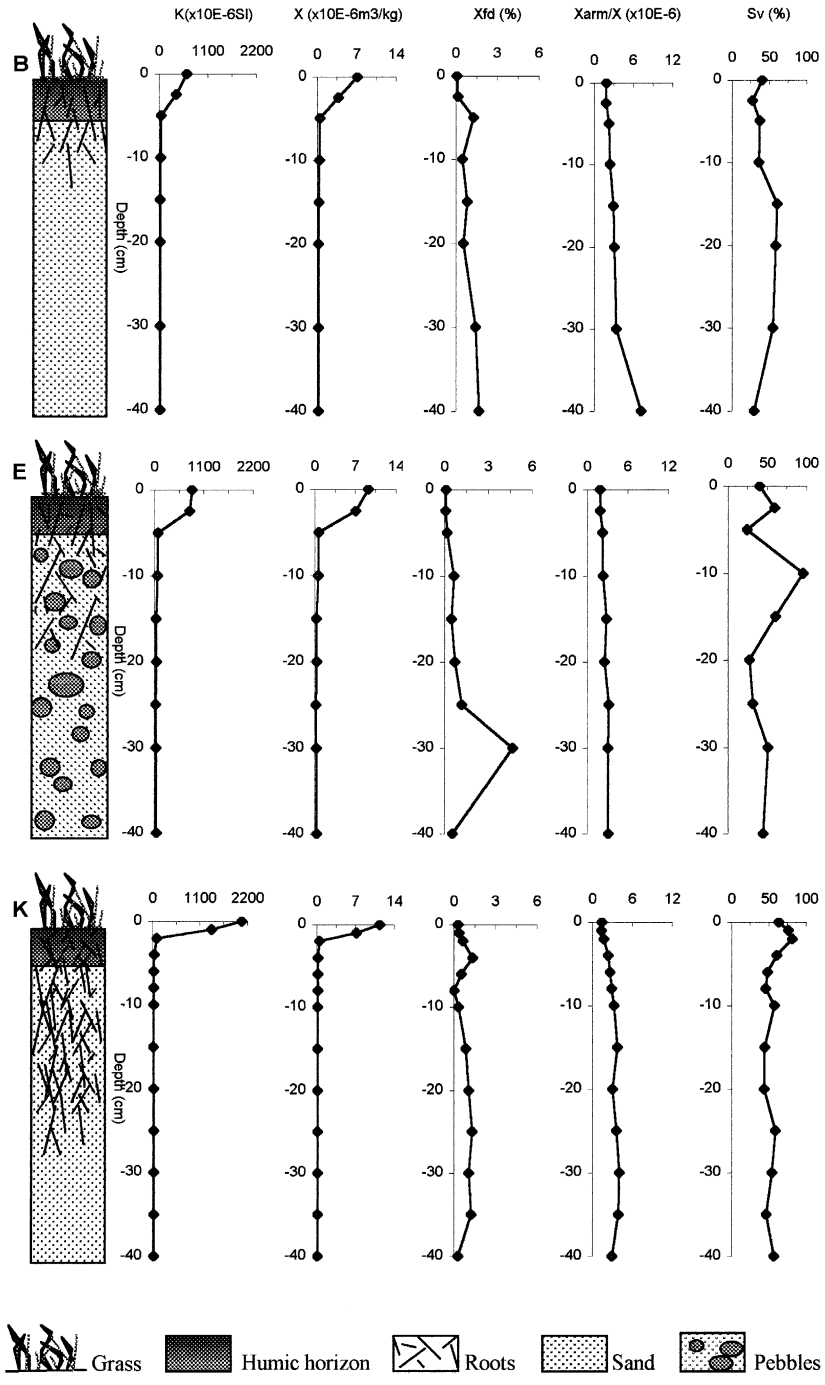


Fig. 5.1. Magnetic parameters for profiles B, E and K.

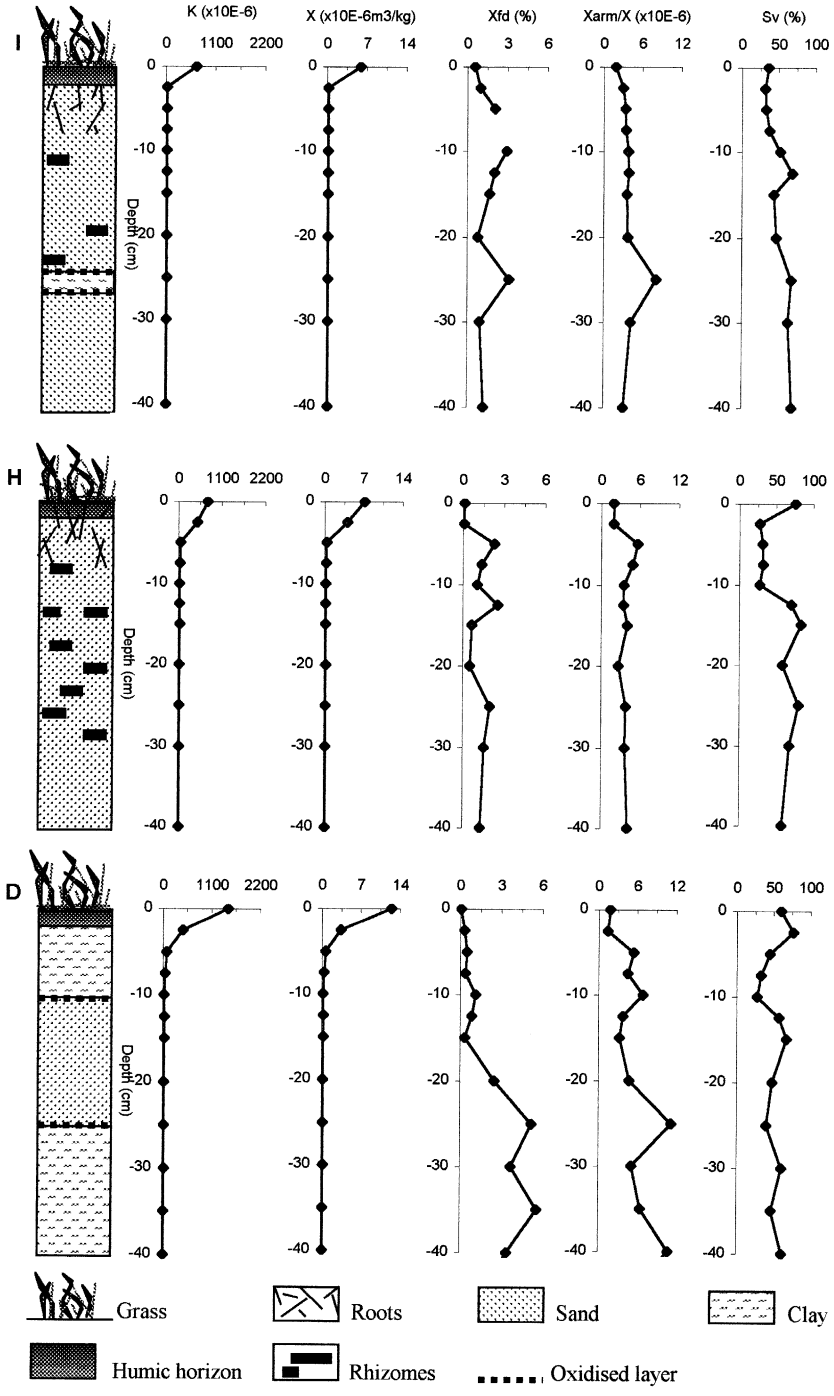


Fig. 5.2. Magnetic parameters for profiles I, H and D.

Table 1
Mineralogical composition of surface soil samples (K excluded), using X-ray analysis

Family	Mineral name	Formula	Profile B	Profile D	Profile E	Profile H	Profile I
Iron oxides	Magnetite	Fe_3O_4	×	×	×	×	
	Maghemite	γ-Fe_2O_3		×			×
	Hematite	α-Fe_2O_3	×	×	×	×	×
Iron sulphides	Pyrite	FeS_2	×	×		×	
Sulphates	Gypsum	$CaCO_4 \cdot 2H_2O$		×		×	
Halides	Halite	NaCl		×		×	×

11.17×10^{-6} SI at -25 cm and 10.72×10^{-6} SI at -40 cm (Fig. 5.2), local increase indicates a decrease in the effective grain size.

3.2.2.4. Viscosity coefficient Sv (%). Sv (%) values vary significantly along each profile and not in the same way as the previous magnetic parameters. Normalised viscosity coefficient Sv (%) is high, usually above 40%, sometimes reaching 80% in profiles H, D and K (Figs. 5.1 and 5.2), and up to 95% in profile E (Fig. 5.1).

The relatively low Sv values in the uppermost levels of profiles B, I and H lead to conclude to higher magnetic hardness in contrast with topsoil of profiles D, E and K (Figs. 5.1 and 5.2). Higher Sv values in intermediate depths are probably due to an enhanced MD content in these parts of the profiles. These MD particles are probably of detrital origin, since pedogenic growth from SP to MD size is not favoured at the bottom of the profiles.

3.2.2.5. Normalised AF demagnetisation curves of ARM. Saturation ARM was not achieved before 100 mT, pointing to the dominant role of magnetically hardness ferrimagnetic minerals (Fig. 6).

In theory, high median destructive fields (MDF_{ARM}) characterise samples with a high percentage of fine SD grains, whereas low median destructive fields are characteristic of coarse MD grains.

AF demagnetisation of ARM is characterised by curves of nearly identical shapes, with MDF_{ARM} values in the narrow range of 25–40 mT for profiles D, E and I (Fig. 6). Profiles D and I contain clayey and sandy horizons (Figs. 5.1 and 5.2). The upper limit of the median field could be generated by clayey particles smaller (as sample D-10) than sand grain. The grain-size distribution in profile E is very heterogeneous (Fig. 5.1) and could also explain the wide range of MDF_{ARM} values. The range of MDF_{ARM} values is more restricted in profiles B, H, K (values centred around 30 mT). This could be due to the sandy nature of the profiles under the humic horizon.

In all the profiles, the lower limit of the median field is for surface samples. This appears clearly for profile I: the curves corresponding to samples at 0 and -2.5 cm (I-0 and I-2.5) are separated from the others. These results seemed to confirm the presence of large grains coming from metallurgical dust fallout at the top of all soil profiles.

4. Biplots

Biplots (combination of two magnetic parameters) can be a useful qualitative technique for the identification of the properties of certain minerals and domain states.

4.1. VRM versus volume susceptibility κ in soil samples

Surface soil samples exhibit higher susceptibilities than nonpedogenic and bottom soil samples (Fig. 7). Volume susceptibility values are around 800×10^{-6} SI for surface samples, whereas the range of κ is between 16.63×10^{-6} (sample K-25) and 39.51×10^{-6} SI (sample D-7.5) for bottom samples.

Most topsoil samples plot in a distinct field, although few plot near bottom samples. This is particularly the case for samples localised at the bottom of

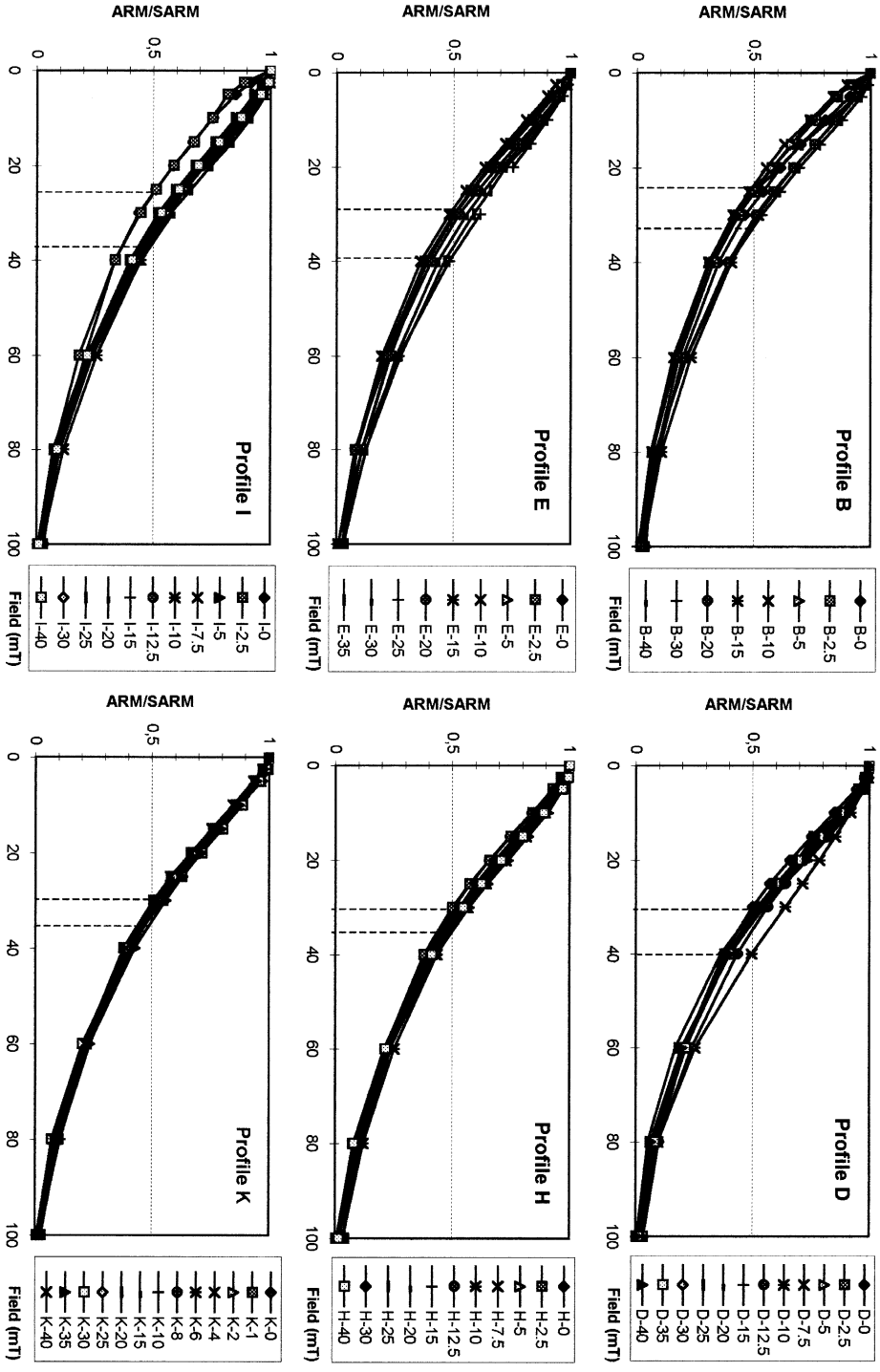


Fig. 6. Normalised AF demagnetisation curves of ARM.

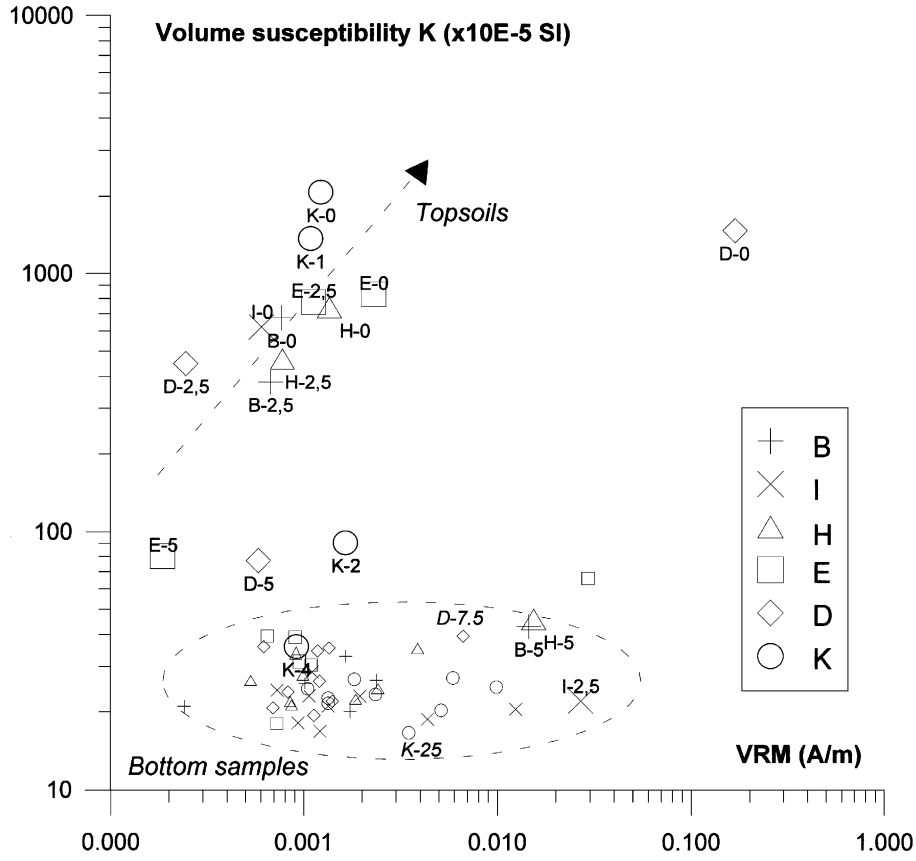


Fig. 7. VRM versus volume susceptibility κ for soil samples. Big size symbols represent topsoil samples and correspond to the humic horizon. Small size symbols represent all other samples. Numbers indexed are the depth of topsoil samples in centimetres. No NRM was acquired for dust samples.

the humic horizon (B-5, H-5, I-2.5, D-5 and K-4). These outliers could be easily explained by pedogenic history.

4.2. $ARM_{40\ mT}$/SARM ratio versus $IRM_{-100\ mT}$/SIRM ratio for the various sets of samples

In Fig. 8, magnetic ratios are represented since ratios largely eliminate the effects of magnetic concentration.

The ratio of $IRM_{-100\ mT}$/SIRM enables to distinguish a ferrimagnetic pole from an antiferromagnetic pole. Ratio values are close to -1 for surface soil samples and atmospheric dusts. Thus, the sample mineralogy is dominated by ferrimagnetism for which saturation is obtained at -100 mT field. The $ARM_{40\ mT}$/SARM ratio is used to determine the grain-size variability of the sample set. Fine grains are characterised with ratio values close to 1 (a high percent of magnetisation remains after the demagnetisation at an alternating field of 40 mT). In contrast, coarse grains are characterised with ratio values close to 0 (only a low percentage of magnetisation).

The values of $ARM_{40\ mT}$/SARM ratio ranged between 0.30 and 0.50. At the exception of sample B-10, the lowest values are obtained for topsoil samples. The highest values are measured in dust samples. Consequently, even if the high magnetic susceptibility values in topsoils have a metallurgical

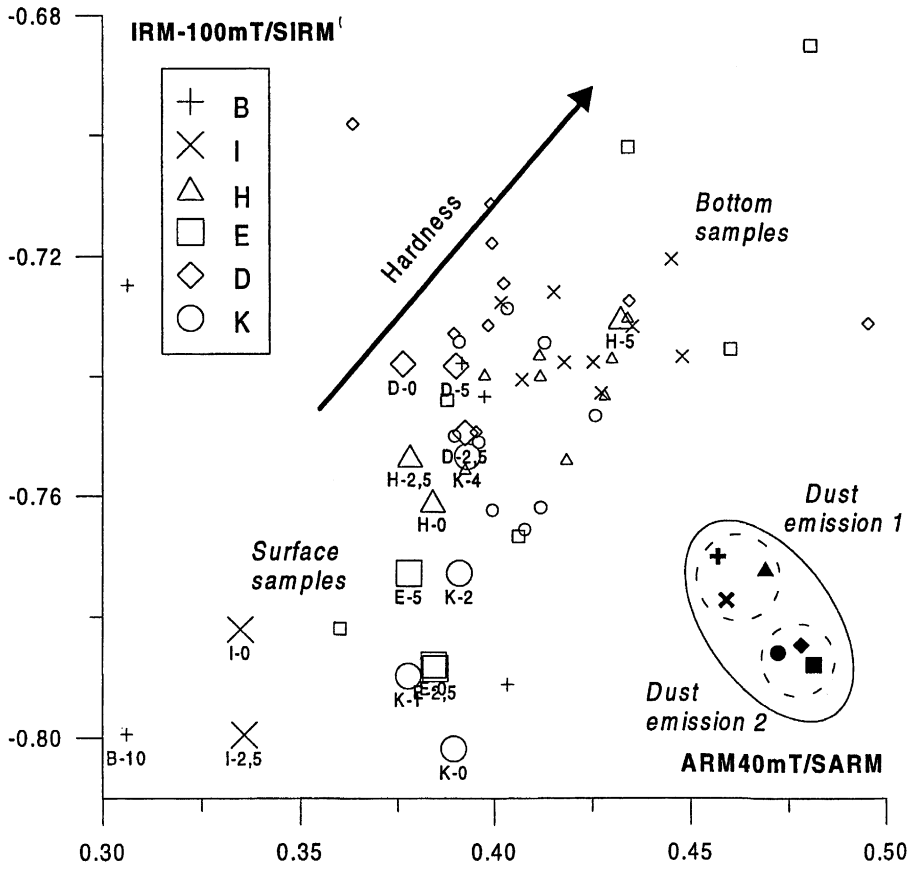


Fig. 8. $ARM_{40\ mT}$/SARM ratio versus $IRM_{-100\ mT}$/SIRM ratio for all samples. Soil profile samples are symbolised as in Fig. 7. Full symbols are used for dust samples.

origin (dust fallout), the distribution/concentration of magnetic minerals in these soil profiles is partly due to pedogenic processes.

Two groups of dust samples can be isolated. One group corresponds to dusts trapped at profiles B, I and H, and the second group is composed of dusts trapped at profiles K, D and E. Thus $ARM_{40\ mT}$/SARM ratio versus $IRM_{-100\ mT}$/SIRM ratio can differentiate the two different contamination emission sources (Fig. 2). As the main wind is "mistral", the first group is directly leeward of the emission source one, whereas the second group is directly submitted to dust fallout of source two. These results confirm the previous observations from Oldfield et al. (1985) and suggest that magnetic parameters can be a useful tool in characterising atmospheric dusts derived from different sources.

This differentiation is not obvious in surface soil samples. The reason is that dusts collected are a "snapshot", whereas soils are an averaged signal. Moreover, dusts were not in contact with soils (salt or not), and therefore, magnetic minerals were not available for inevitable chemical transformation.

4.3. $IRM_{-20\ mT}$/SIRM ratio versus $IRM_{-200\ mT}$/SIRM ratio for the various sets of samples

The contrast between topsoil samples and bottom samples illustrated in Fig. 9 is consistent with a proportionally much higher hard magnetic component in bottom samples.

The range of variation in the lower reverse field ratio is rather small (0.4 units) and does not clearly differentiate topsoil samples from dust samples.

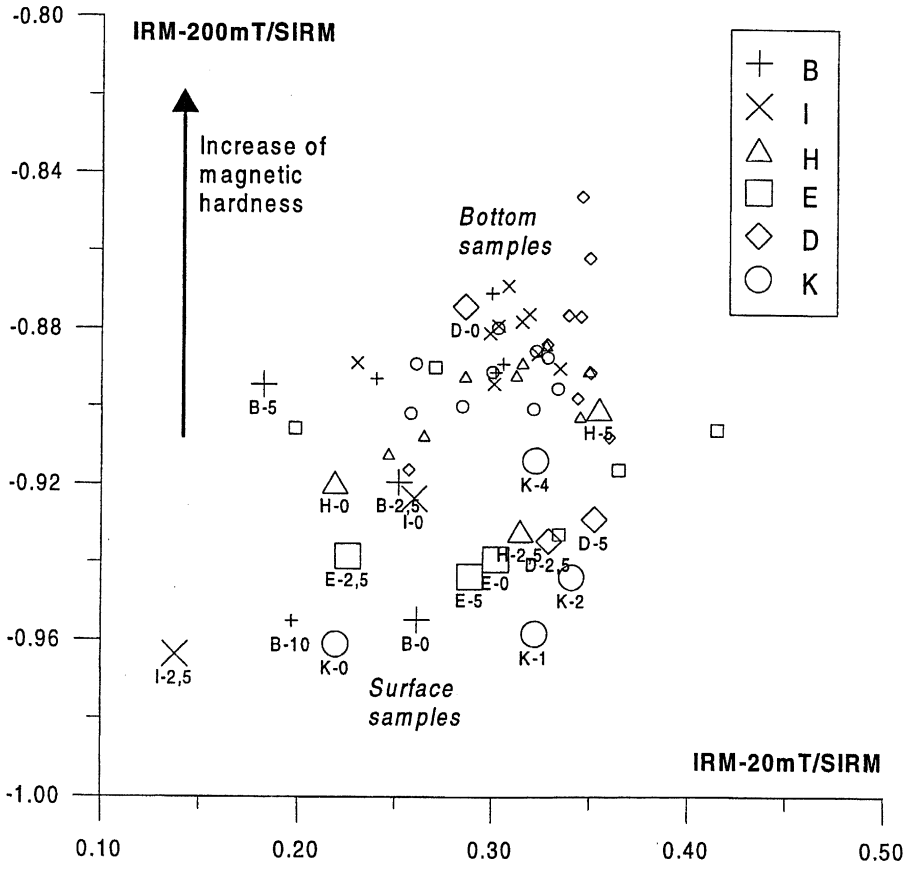


Fig. 9. $IRM_{-20\ mT}/SIRM$ ratio versus $IRM_{-200\ mT}/SIRM$ ratio for all samples. Both soil and dust samples are symbolised as in Fig. 8.

However, the high reverse field ratio discriminates the sample sets more effectively.

5. Conclusions

Measurements of soil magnetic susceptibility can be rapidly carried out at low cost, both in field and in laboratory, and can be easily used to trace the extent of soil contamination in industrialised areas.

The susceptibility map obtained appears to represent the distribution of deposited metallurgical fallout over the salt-marsh area concerned. Obviously, magnetic parameters measured in salt-affected soils reflect several effects. The influence of metallurgical emissions as the main source of magnetic particles tends to mask other possible sources. Magnetic susceptibility variations can be explained not only by atmospherically deposited dust but also by postdepositional weathering and/or formation of magnetic phases by pedogenic processes (Zheng et al., 1991; Zhou et al., 1990).

Our conclusions can be summarised as follows.

(1) The main fact confirming the presence of metallurgical dusts in topsoil is very low frequency-dependent susceptibility (0.5%). The other parameter consistent with aeolian contamination signal is median destructive field. Low values are characteristic of coarse MD grains and were observed in surface samples.

(2) Size discrimination between surface soil samples and dust is clear (Fig. 8). Trapped dust particles have apparently smaller sizes than topsoil samples.

(3) An increase of magnetic hard component from topsoil towards the bottom of the profiles is evi-

denced (Fig. 9). Humic horizons are dominated by anthropogenic MD magnetite with some maghemite, whereas the predominant remanence carriers in many modern soil are natural SD magnetite (Maher, 1986; Fine et al., 1989, 1993; Singer and Fine, 1989). These data come from gley layers, which might be expected to remove fine magnetite through dissolution (Maher, 1986; Thompson and Oldfield, 1986).

(4) The soil of this area is seasonally subject to wet–dry cycles, and thus, the character of the pedogenic magnetite would probably be influenced by the duration and intensity of each wet and dry phase. Likewise, magnetite is favoured in less oxidising conditions (although it may be removed with prolonged reduction), and hematite is common in more oxidising conditions although they can coexist (Maher, 1986; Thompson and Oldfield, 1986).

Acknowledgements

This paper is the contribution no. 208 of CNRS-INSU PROSE 97 research program. Eduard Petrovsky is thanked for his suggestions on the manuscript.

References

Afnor, 1973. Pollution atmosphérique-Mesure des “retombées” par la méthode des “plaquettes de dépôt” (Measurement of atmospheric fallout by means of metal plaquettes). Norme française homologuée X 43.00.

Baiz, D., Rossignol, J.P., 1995. Référentiel pédologique 1995. Ed. INRA, Paris, France, pp. 95–98.

Dearing, J.A., 1994. Environmental Magnetic Susceptibility: using the Bartington MS2 system. Bartington Instrument. Chi Publishing, Kenilworth, UK, 104 pp.

Dearing, J.A., Dann, R.J.L., Hay, K., Lees, J.A., Loveland, P.J., Maher, B.A., O’Grady, K., 1996. Frequency-dependent susceptibility measurements of environmental materials. Geophys. J. Int. 124, 228–240.

Dekkers, M.J., Pietersen, H.S., 1992. Magnetic properties of low-Ca fly ash: a rapid tool for Fe-assessment and a survey for potentially hazardous elements. In: Glasser, F.P., McCarthy, G.J., Young, J.F., Mason, T.O., Pratt, P.L. (Eds.), Advanced Cementitious Systems: Mechanisms and Properties. Materials Research Society Symposium Proceedings, vol. 245, Materials Research Society, Pittsburgh, pp. 37–47.

Durza, O., 1999. Heavy metals contamination and magnetic susceptibility in soils around metallurgical plant. Phys. Chem. Earth (A) 6, 541–543.

Fine, P., Singer, M.J., La Ven, R., Verosub, K., Southard, R.J., 1989. Role of pedogenesis in distribution of magnetic susceptibility in two California chronosequences. Geoderma 44, 287–306.

Fine, P., Singer, M.J., Verosub, K., 1992. Use of magnetic susceptibility measurements in assessing soil uniformity in chronosequence studies. Soil Sci. Soc. Am. J. 56, 1195–1199.

Fine, P., Singer, M.J., La Ven, R., Verosub, K., TenPas, J., 1993. New evidence for the origin of ferrimagnetic minerals in loess from China. Soil Sci. Soc. Am. J. 57, 1537–1542.

Flanders, P.J., 1994. Collection, measurements and analysis of airborne magnetic particulates from pollution in the environment. J. Appl. Phys. 75, 5931–5936.

Flanders, P.J., 1999. Identifying fly ash at a distance from fossil fuel power stations. Environ. Sci. Technol. 33, 528–532.

Forster, Th., Evans, M.E., Heller, F., 1994. The frequency dependence of low field susceptibility in loess sediments. Geophys. J. Int. 118, 636–642.

Gaucher, G., Burdin, S., 1974. Géologie, géomorphie et hydrologie des terrains salés. Ed. Presses Universitaires de France, Paris, France, 229 pp.

Hanesch, M., Petersen, N., 1999. Magnetic properties of a recent parabrown-earth from southern Germany. Earth Planet. Sci. Lett. 169, 85–97.

Hansen, L.D., Silberman, D., Fisher, G.L., 1981. Crystalline components of stack-collected, size-fractionated coal fly-ash. Environ. Sci. Technol. 15, 1057–1062.

Hay, K.L., Dearing, J.A., Baban, S.M.J., Loveland, P.J., 1997. A preliminary attempt to identify atmospherically derived pollution particles in English topsoils from magnetic susceptibility measurements. Phys. Chem. Earth 22, 207–210.

Heller, F., Strzyszcz, Z., Magiera, T., 1998. Magnetic record of industrial pollution in forest soils of Upper Silesia, Poland. J. Geophys. Res. 103, 17767–17774.

Hunt, A., Jones, J., Oldfield, F., 1984. Magnetic measurements and heavy metals in atmospheric particulates of anthropogenic origin. Sci. Total Environ. 33, 129–139.

Jordanova, D., Jordanova, N., 1999. Magnetic characteristics of different soil types from Bulgaria. Stud. Geophys. Geod. 43, 303–318.

Jordanova, D., Petrovsky, E., Jordanova, N., Evlogiev, J., Butchvarova, V., 1997. Rock magnetic properties of recent soils from northeastern Bulgaria. Geophys. J. Int. 128, 474–488.

Kapicka, A., Jordanova, N., Petrovsky, E., Ustjak, S. Magnetic stability of power-plant fly ash in different soil solutions. Phys. Chem. Earth., in press.

Lecoanet, H., Lévêque, F., Segura, S., 1999a. Magnetic susceptibility in environmental applications: comparison of field probes. Phys. Earth Planet. Inter. 115, 191–204.

Lecoanet, H., Lévêque, F., Ambrosi, J.P., 1999b. Magnetism and geochemistry of soils contaminated by iron industry emissions. Actes du 2ème Colloque de Géophysique des Sols et des Formations Superficielles. Geofcan, BRGM, Orléans, France, pp. 139–144.

Magiera, T., 1998. Podatność magnetyczna gleb Pienińskiego Parku Narodowego jako efekt antropogenicznych zanieczys-

czczeń atmosfery. [Soil magnetic susceptibility in the Pieniny National Park as a result of anthropogenic air pollution] Przyroda Cztowiek 6, 125–136.

Maher, B.A., 1986. Characterisation of soils by mineral magnetic measurements. Phys. Earth Planet. Inter. 42, 76–92.

Mitchell, R.S., Sluskoter, H.J., 1976. Mineralogy of ash of some American coals. Fuel 55, 90–96.

Mullins, C.E., 1977. Magnetic susceptibility of the soil and its significance in soil science–a review. J. Soil Sci. 28, 223–246.

Oldfield, F., Hunt, A., Jones, M.D.H., Chester, R., Dearing, J.A., Olsson, L., Prospero, J.M., 1985. Magnetic differentiation of atmospheric dusts. Nature 317, 516–518.

Petrovsky, E., Ellwood, B., 1999. Magnetic monitoring of water, air and land pollution. In: Maher, B., Thompson, R. (Eds.), Quaternary Climate, Environment and Magnetism. Cambridge Univ. Press, Cambridge, U.K., pp. 279–322.

Shu, J., Dearing, J.A., Morse, A.P., Yu, L., Li, C. Magnetic properties of daily sampled total suspended particulates in Shanghai. Environ. Sci. Technol., in press.

Singer, M.J., Fine, P., 1989. Pedogenic factors affecting magnetic susceptibility of Northern Californian soils. Soil Sci. Soc. Am. J. 53, 1119–1127.

Strzyszcz, Z., Magiera, T., 1996. The influence of industrial emissions on the magnetic susceptibility of soil in upper Silesia. Stud. Geophys. Geod. 40, 276–286.

Thompson, R., Oldfield, F., 1986. Environmental Magnetism. Allen and Unwin, London, 227 pp.

Zheng, H.B., Oldfield, F., Yu, L., Shaw, J., An, Z., 1991. The magnetic properties of particle-sized samples from the Luo Chuan loess section: evidence for pedogenesis. Phys. Earth Planet. Inter. 68, 250–258.

Zhou, L.P., Oldfield, F., Wintle, A.G., Robinson, S.G., Wang, J.T., 1990. Partly pedogenic origin of magnetic variations in Chinese loess. Nature 346, 737–739.